

Manuscript submitted to *J. Phys. Chem. A*

**Action spectroscopy of gas-phase carboxylate anions by multiple photon
IR electron detachment/attachment**

Jeffrey D. Steill and Jos Oomens*

FOM Institute for Plasma Physics 'Rijnhuizen', Edisonbaan 14, 3439MN Nieuwegein,
The Netherlands

*Corresponding author: joso@rijnhuizen.nl

Abstract.

We report on a form of gas-phase anion action spectroscopy based on infrared multiple photon electron detachment and subsequent capture of the free electrons by a neutral electron scavenger in a Fourier Transform Ion Cyclotron Resonance (FTICR) mass spectrometer. This method allows one to obtain background-free spectra of strongly bound anions, for which no dissociation channels are observed. The first gas-phase spectra of the acetate and propionate anions are presented using SF₆ as electron scavenger and a free electron laser as source of intense and tunable infrared radiation. To validate the method, we compare infrared spectra obtained through multiple photon electron detachment/attachment and multiple photon dissociation for the benzoate anion. In addition, different electron acceptors are used, comparing both associative and dissociative electron capture. The relative energies of dissociation (by CO₂ loss) and electron detachment are investigated for all three anions by DFT and CCSD(T) methods. DFT calculations are also employed to predict vibrational frequencies, which provide a good fit to the infrared spectra of the propionate and acetate anions. The frequencies of the symmetric and asymmetric carboxylate stretching modes for the aliphatic carboxylates are compared to those previously observed in condensed phase IR spectra and benzoates, showing a strong influence from the solution environment and a slight substituent effect on the asymmetric stretch.

KEYWORDS: electron detachment, action spectroscopy, multiple photon excitation, acetate, propionate, gas phase

Introduction.

Spectroscopy of gas-phase molecular ions through multiple photon IR absorption-induced dissociation is well characterized (see e.g. several recent review articles).¹⁻³ The high intensity provided by infrared lasers and rapid intramolecular redistribution of vibrational energy (IVR) in polyatomic molecules allow for multiple-photon absorptions at IR-active resonances, creating high internal energies. For anions, the increased internal energy can result in either dissociation or electron detachment,⁴⁻⁶ since electron detachment energies are typically comparable to bond dissociation energies. For anions that lack an easily energetically or entropically accessible dissociation channel, the electron detachment channel may dominate. Multiple photon infrared dissociation is not always expected for small molecules which lack the many vibrational degrees of freedom that allow molecules to efficiently acquire internal energies above their dissociation threshold. Thus, small molecular anions are an interesting class of gas-phase ions to be studied with IR multiple photon detachment spectroscopy.

Several infrared action spectroscopy methods based on electron ejection have been developed over the last decades. Infrared autodetachment spectroscopy has been applied to study the spectroscopy of anions with relatively low electron affinities. Excitation of a vibrational band, usually in the hydrogen stretching region, which couples to the electron continuum leads to resonances in the autodetachment of the electron. Systems studied using this method include the imidogen anion⁷ (NH⁻), the nitromethane anion⁸ and

anionic water clusters.⁹ IR multiple photon induced ejection of electrons has been observed for neutral species for which the dissociation threshold is higher than the ionization potential, such as fullerenes and metal clusters. In combination with a free electron laser, this process has been used as a spectroscopic tool by mass-selective detection of the resulting cations.¹⁰ Infrared multiple photon detachment of molecular anions has also been reported^{4,11}. Brauman and coworkers reported the infrared multiple photon electron detachment of the benzyl anion,⁴ where the detached electron was detected using CCl_4 as electron scavenger forming Cl^- . The method could however not be used as a spectroscopic technique since no sharp spectral features were observed. Also the experiment by Beauchamp¹¹ on isomers of C_7H_7^- appears to suffer from the limited tuning range of a CO_2 laser, which results effectively in only one observable IR band for two isomers. Recently, in an infrared multiple photon absorption experiment on the SF_5^- ion performed in a Fourier Transform ion-cyclotron resonance (FTICR) mass spectrometer, the formation of SF_6^- was observed upon resonance, due to capture of the detached electrons by residual neutral SF_6 in the ICR cell.¹² Photodetachment experiments performed in FTICR mass spectrometers are facilitated by the use of electron attaching molecules, since the cyclotron frequency of free electrons is much too high for conventional detection. The use of SF_6 , CCl_4 and other gases as free electron capture agents is common. The use of molecules with large electron capture cross-sections is often referred to as the electron scavenger technique and a thorough description of this method is given by Kohan *et al.*¹³ The application of this method to the infrared is limited, however. It is anticipated that infrared irradiation of molecules of small to moderate size with comparable dissociation and detachment energies may show a

competition between the two channels, and this is explored here as a means of gas-phase infrared action spectroscopy. As an example, we study the infrared spectra of the small aliphatic carboxylate anions acetate and propionate, as well as that of the benzoate anion, which was recently investigated with IR multiple photon dissociation spectroscopy.¹⁴

The IRMPD spectrum of the benzoate anion was obtained by monitoring the appearance of the phenide, $C_6H_5^-$, anion produced by CO_2 loss of the parent, and DFT calculations provide a good fit to the spectrum. The infrared spectrum of the gas-phase benzoate anion serves as a useful reference for the symmetric and asymmetric carboxylate stretching frequencies, denoted v_s and v_a , respectively. The splitting between these two prominent spectral bands, denoted Δv_{a-s} , is often used as a diagnostic, providing a measure of the relative strength of counterion binding to the carboxylate moiety in gas-phase clusters, solutions and salts. A comparison of the benzoate frequencies to those of aliphatic carboxylates is desirable because it provides some measure of the effect of resonance stabilization on the carboxylate stretching frequencies. However, the small size and hence the low state densities of the aliphatic carboxylate anions acetate and propionate make it impossible to measure their infrared spectra by the same methods as the benzoate anion. Condensed phase IR spectra of the acetate¹⁵⁻¹⁷ and propionate^{15,18} anions as sodium salts and in aqueous solution have been reported but a gas-phase spectrum is required for determination of the inherent, unperturbed vibrational frequencies of these ions. As was shown in the previous study of the benzoate anion, the carboxylate stretch frequencies are significantly shifted in condensed phase spectra compared to the gas phase.

Gas-phase studies of the acetate, propionate and benzoate anions have been performed using anion photoelectron spectroscopy. Ideally, the anion photoelectron spectrum provides a measure of the vertical and adiabatic electron affinities, as well as structural information and analysis of the stability of the neutral species. Woo *et al.* studied the benzoate anion by this technique, determining the adiabatic electron detachment energy to be 3.4-3.6 eV.¹⁹ Similarly, the acetate anion was studied by Lu and Continetti²⁰ and Wang and co-workers²¹⁻²³ yielding an adiabatic electron affinity of the acyloxy radical of 3.47 eV²⁰ to 3.25 eV.²³ The low-temperature experiments of Wang *et al.* are expected to be the most reliable and thus the value of 3.25 eV can be considered an improved value. Experiments of X.B. Wang and co-workers show that the propionate anion has an adiabatic electron detachment energy quite similar to that of the acetate anion.²²

The thermodynamics of electron detachment are relevant because the detachment channel may compete with the CO₂ loss dissociation channel for these small carboxylate anions. The dynamics of intramolecular energy transfer likely play a primary role, but the thermodynamic values provide a foundation for discussion of the competition between the detachment and dissociation channels. Lu and Continetti²⁰ examined this process for acetate by using thermodynamic cycles based upon experimental values, and determined a dissociation energy of 2.48(0.06) eV, which compares favorably to the collision-induced dissociation experiments of Wenthold and Squires²⁴ yielding a value of 2.5(0.11) eV. Thus, while the energy of CO₂ loss is smaller than the electron detachment energy,

the two processes are similar enough in energy that they can be expected to compete upon infrared irradiation.

Experimental Methods.

Benzoate, propionate and acetate ions are generated by electrospray ionization of 1mM solutions of the corresponding acids in a 80:20 MeOH:H₂O solvent mix. A small amount of NaOH_(aq) was added to raise the pH and facilitate deprotonation of the analytes.

Ionization with a Micromass “Z-spray” electrospray ionization (ESI) source and subsequent storage and isolation in the Penning trap of a homebuilt Fourier-Transform Ion Cyclotron Resonance Mass Spectrometer²⁵ (FTICR-MS) has been described previously.²⁶ Infrared radiation in the range of 5.5 to 11 μ m is generated by the free-electron laser located at the FOM Institute for Plasma Physics, Rijnhuizen, (FELIX)²⁷.

The ions are irradiated for 3 seconds at a macropulse repetition rate of 5 Hz, with 3 mass spectra averaged per spectral data point. The background pressure in the cell without an electron capture gas was 5×10^{-8} Torr. With addition of the background electron scavenger gases SF₆ and CH₃I, the ICR cell pressure increased to approximately 2×10^{-7} Torr.

Minimum energy geometries and harmonic vibrational frequencies were computed by DFT and *ab-initio* methods implemented within Gaussian03.²⁴ All structures were verified to be true minima on the potential energy surface by harmonic frequency calculations. For acetate and propionate the optimization and harmonic vibrational

frequency calculations were performed at multiple conformations to verify minimum energy configurations. Energies of electron detachment and dissociation by CO₂ loss for all carboxylates were investigated using DFT (B3LYP) and Coupled-Cluster (CCD and CCSD(T)) methods. For the CCSD(T) calculations, energies are computed at the B3LYP/aug-cc-pVDZ geometries. Zero-point energy corrections are applied to the thermodynamic parameters (zero degrees Kelvin) at the level of theory used, except for CCSD(T) values, which are corrected according to the unscaled B3LYP/aug-cc-pVDZ harmonic vibrational frequencies. Aqueous solution-phase vibrational frequency calculations were carried out using the Onsager dipole-dipole sphere self-consistent reaction field model implemented with a spherical radius of 3.44, 3.74 and 4.30 Å for acetate, propionate, and benzoate respectively.

Results and Discussion.

A. Benzoate Anion Dissociation and Detachment.

As in our prior studies on the benzoate anion¹⁴ (C₆H₅COO⁻), the primary photodissociation product observed was the phenide anion, C₆H₅⁻, resulting from loss of CO₂. Resonant dissociation was found to correlate well with DFT anharmonic and scaled harmonic frequency calculations. Addition of a small amount of SF₆ background gas to the ICR cell reveals an additional photodecomposition channel. As shown in Figure 1, in addition to dissociation, detachment is observed via observation of the SF₆⁻ anion due to associative electron attachment. The well-known electron capture behavior of SF₆

provides an effective means for detecting the electron detachment channel. The spectral bands from the photodetachment channel clearly correlate with those observed from depletion of the $\text{C}_6\text{H}_5\text{COO}^-$ intensity and dissociation into the C_6H_5^- channel.

To verify the phenomenon observed is in fact due to electron capture by the background gas, a separate electron capture agent is used, in this case methyl iodide. The electron capture cross section of methyl iodide is less than that of SF_6 at low electron energies, but little difference is observed in the scavenger yield since the photodetached electrons remain trapped in the ICR cell, resulting in effectively equivalent collection efficiencies. Dissociative electron attachment to CH_3I to produce I^- ions is shown overlaid with the associative electron attachment to SF_6 in Figure 2. The benzoate infrared resonances clearly correlate for both electron scavengers, demonstrating the generality of the method.

Scavengers resulting in an atomic anion from dissociative electron attachment such as CH_3I and CCl_4 have the advantage that the reaction product does not interact with the IR radiation, whereas anionic SF_6 could undergo dissociation as a result of IR absorption. We have recently measured the IRMPD spectrum¹² of SF_6^- and the only substantial dissociation was found in the region $600\text{-}800\text{ cm}^{-1}$, which produced essentially only SF_5^- . Experimentally, the use of SF_6 as an electron scavenger was often found to give more stable signals because of its higher vapor pressure and inherently more constant background pressure over the course of an IR scan. There was no appreciable SF_5^- signal observed, which suggests that the photodetached electrons are of very low energy.

B. Acetate and Propionate Detachment Spectroscopy.

Unlike the benzoate anion, irradiation of acetate and propionate anions does not show any detectable dissociation products under our experimental conditions. However, as shown in Figures 3 and 4, the appearance of SF_6^- results from associative attachment of detached electrons to the background SF_6 gas. Thus, the detachment channel provides a means for infrared action spectroscopy of these ions that are not otherwise measurable. The infrared spectra of both ions show clear resonances attributable to the symmetric and asymmetric carboxylate stretching modes. The vibrational spectrum is compared to DFT anharmonic and scaled harmonic frequency calculations, and agreement is reasonable for both anions, with scaled harmonic B3LYP/aug-cc-pVDZ methods showing good overall agreement. The peak positions of the symmetric and asymmetric carboxylate stretches for acetate are observed at 1305 and 1590 cm^{-1} , respectively (Figure 3). In addition, the OCO bending mode is also clearly discernable at 835 cm^{-1} . Although the propionate anion is larger than acetate, no dissociation was observed for this anion either. However, as shown in Figure 4, the electron detachment channel produced a clear spectral signature of the carboxylate symmetric and asymmetric stretching modes at 1305 and 1600 cm^{-1} , respectively, as well as the OCO bending mode at 815 cm^{-1} .

The frequency values of the symmetric and asymmetric carboxylate stretches for benzoate, acetate and propionate are shown in Table 1. Gas-phase values obtained here are compared to literature values obtained from condensed-phase experiments. It is clear

that the condensed-phase experiments show significantly different values for these vibrations, and the calculated values correlate well with the gas-phase experiments. The energy difference between the symmetric and asymmetric carboxylate stretches for acetate is somewhat smaller than that observed for the benzoate anion.¹⁴ The splitting between the carboxylate stretching frequencies for the propionate anion is also somewhat smaller than that for benzoate, but slightly less so. An increase to higher values of the COO^- asymmetric stretch is commonly observed upon addition of an electron withdrawing group in aromatic^{14,29} and aliphatic¹⁵ carboxylates. Thus the observation of a lower value for the asymmetric stretch for the aliphatic carboxylates as compared to benzoate is interpretable as due to the relative electron donating tendency of the alkyl group.

Harmonic frequency calculations provide a means for assignment of the observed spectral features to specific vibrational modes of acetate and propionate, but require confident determination of minimum energy configurations. To this end, both DFT and *ab initio* methods are employed with various basis sets. The geometry optimizations proceed to multiple stationary points on the potential energy surface, which are connected through internal rotations about the C-C single bonds of acetate and propionate. The energy difference between two C_s symmetry structures of acetate is small, as is expected, in the range of a few meV or less as calculated by DFT, CCD and CCSD(T) methods. CCSD(T)/aug-cc-pVDZ and CCSD(T)/6-311++G** single-point energy calculations performed at the B3LYP/aug-cc-pVDZ optimized structures for each of these conformations show an energy difference of -0.7 and 1.5 meV, respectively. Such

differences are negligible at the temperature of the experiment (293 K) and moreover, the predicted IR spectrum is similar for the two rotamers.

For propionate there are four possible structures of C_s symmetry connected by internal rotations about each of the C-C bonds. According to B3LYP/aug-cc-pVDZ calculations, three of these four stationary structures show imaginary frequencies, reducing to a global minimum of C_s symmetry, which is shown in Figure 4. There is some disagreement between basis sets among the DFT calculations, however, as the 6-311++G** basis set produces an imaginary frequency at this geometry and optimizes to a structure of C_1 symmetry with the methyl hydrogens staggered slightly such that the H-C-C-C-O plane is destroyed. This lowered-symmetry result is also reproduced with the CCD calculations using all but the aug-cc-pVDZ basis set. To examine the energetic difference between the C_s and C_1 symmetry structures, CCSD(T) single point energy calculations were performed at each of the optimized structures. CCSD(T) calculations using the 6-311++G** and the aug-cc-pVDZ basis sets show the C_s symmetry structure to be lower in energy by 0.1 and 30 meV, respectively. Again, the energy difference between the conformations is minimal, and the effect on the predicted IRMPD spectrum negligible.

The best overall spectral agreement is seen with the DFT method using the aug-cc-pVDZ basis set, scaled by a factor of 0.98, for both propionate and acetate. These calculations overestimate the values for the observed symmetric COO^- stretch and also very slightly for the asymmetric COO^- stretch. The CCD method with the same basis set scaled by a factor of 0.95 overestimates these bands as well, and in most cases even more so. The

gas-phase frequencies for these vibrational modes are sufficiently shifted relative to the condensed phase to warrant some computational investigation of the solution spectra.

As shown in Table 1, the B3LYP/aug-cc-pVDZ harmonic vibrational frequency calculations performed using the Onsager dipole-dipole model of aqueous solution reproduce these shifts qualitatively if not quantitatively. The red-shift in the asymmetric stretch in aqueous solution is accounted for well by the model, but the blue-shift in the symmetric stretch is not fully reproduced. This trend is consistent for all the three carboxylate anions studied, suggesting improvement is possible by use of a more sophisticated reaction field model, but demonstrating a general qualitative spectroscopic agreement.

C. Energetics of Decarboxylation and Electron Detachment

In addition to facilitating spectral interpretation, the calculations also provide a foundation for discussion of the relative energies of the dissociation and detachment channels for the three carboxylate anions studied. For the benzoate anion, the B3LYP/aug-cc-pVDZ results were shown to give an accurate spectral prediction, so this method was chosen here for generating optimum structures for higher order *ab initio* energy calculations. The conformational analysis and spectral interpretation performed for acetate and propionate allows for a consistent model framework to treat these three anions, as the DFT calculations provide good agreement with the data and with coupled-cluster calculations. Thus, the optimized B3LYP/aug-cc-pVDZ structure (and zero-point energy correction) from the eclipsed acetate conformer is used for CCSD(T) energy

calculations and as starting points for the optimizations and frequency calculations of the neutral CH_3COO radical. The B3LYP/aug-cc-pVDZ result of C_s symmetry is the starting point for CCSD(T) energy calculations on propionate and for optimizations of the $\text{C}_2\text{H}_5\text{COO}$ radical.

The results of the zero-point energy-corrected electron affinities and decarboxylation energies are shown in Table 2. As seen in Table 2, the calculated energy of direct electron detachment is larger than the decarboxylation energy for all three ions, as both the vertical and adiabatic detachment energies are larger than the dissociation energies. The electron affinities of the $\text{C}_2\text{H}_5\text{COO}$ and CH_3COO radicals are roughly equivalent, and both are smaller than the electron affinity of $\text{C}_6\text{H}_5\text{COO}$ by only a few tenths of an eV. These calculated values compare favorably to the experimentally determined adiabatic detachment energy values for benzoate¹⁹, acetate²⁰⁻²³ and propionate.²² The CH_3COO and $\text{C}_6\text{H}_5\text{COO}$ radicals are calculated to be stable with respect to dissociation, but the $\text{C}_2\text{H}_5\text{COO}$ radical is not, and shows an exothermic dissociation of approximately 0.5 eV to C_2H_5 and CO_2 .

All the anions are stable with respect to CO_2 loss, and the endothermicity of this process is similar for all three anions, but the energy of this process is somewhat greater for propionate than for acetate, and smallest for benzoate. As shown in Table 3, this can be related to the relative stabilities of the anionic fragments, since the electron affinity (EA) of C_6H_5 is about 1 eV, the EA of CH_3 is barely positive, and that of C_2H_5 is negative. Comparison to the electron affinities of the decarboxylated fragment hydrocarbons in

Table 3 shows that the carboxylate group plays a large role in stabilization of the negative charge, especially for the aliphatic carboxylate anions.

These calculated values compare favorably to experimental determinations of the electron affinity of 1.096(.006) eV for the C₆H₅ radical by Gunion *et al.*,³⁰ and a value of 0.08(0.03) eV for the methyl radical determined by Ellison *et al.*³¹ The small electron affinities of the methyl radical and negative electron affinity of the ethyl radical suggest that decarboxylation of the acetate and propionate parent ions would produce short-lived anions on the timescale of the irradiation and detection in these experiments. Thus, while it is likely that the failure to observe dissociation products for acetate and propionate is a manifestation of the intramolecular dynamics in systems with smaller vibrational state densities, it is also possible that the observed electron detachment proceeds through an intermediate decarboxylation step, followed by prompt autodetachment of the resulting hydrocarbon anion. This mechanism would be energetically favored, however, the clear observation of electron detachment from the benzoate anion – despite the significant thermodynamic stability of the phenide dissociation product – suggests that the detachment process can proceed directly from the parent ion.

Conclusions

The smallest aliphatic carboxylates acetate and propionate have been characterized in the gas phase by a novel infrared action spectroscopy method, in which IR absorption is

signaled by detachment of an electron followed by capture of the electron by a scavenger, which is detected in the mass spectrum. DFT calculations yield confirmation of the benchmark frequency values for the splitting of the symmetric and asymmetric carboxylate stretch modes in gas-phase aliphatic carboxylate anions. The splitting for the aliphatic carboxylates is smaller than that of benzoate, presumably due to the greater electron withdrawing effect of the phenyl ring as compared to the methyl and ethyl groups. This effect is consistent with that observed from substituted aromatic and aliphatic carboxylates, where addition of electron-withdrawing groups increases the observed splitting of the bands. As was observed with benzoate, the condensed-phase spectra are significantly shifted relative to the gas-phase spectra.

The method used for spectroscopic detection has been verified by application in the previously characterized benzoate anion for experimental validation. The observation of both dissociation and detachment from the benzoate anion suggests opportunities for investigating the competition between these processes often observed in metastable anionic species. The competition between the rates of these unimolecular reactions is related to the energetic, and possibly also kinetic, differences between the channels. Investigation of the thermodynamic energy differences and prediction of vibrational frequencies were done using DFT and coupled-cluster methods. The electron detachment and decarboxylation energies are shown to be similar for the benzoate, acetate, and propionate ions, so it is suggested that the failure to observe the CH_3^- or C_2H_5^- dissociation products may be due to the thermodynamic instability of the fragment ions

or possibly be a manifestation of the difference in dissociation dynamics for large and small molecular ions.

It is anticipated that this experimental methodology can be easily extended to a wide variety of molecular anions, particularly opening the possibility of infrared action spectroscopy to systems hitherto considered either too small or too rigid for infrared multiple photon dissociation experiments. As an example, we have recently reported the first gas-phase IR spectrum of the C₆₀ anion, which as a consequence of its high stability does not undergo dissociation under our experimental conditions.³² Further investigation of the underlying dynamics may be relevant to studies of metastable anions in general. As shown by many studies of metastable negative ions, small molecular ions can couple vibrational internal energy to the electron detachment channel. The relative success of RRKM/QET statistical formulations suggests the possibility of modeling the competition between the dissociation and detachment within this framework.

Acknowledgment

It is a pleasure to acknowledge the excellent support of Drs. Britta Redlich and Lex van der Meer as well as others of the FELIX staff. This work is part of the research program of FOM, which is financially supported by the Nederlandse Organisatie voor Wetenschappelijk Onderzoek (NWO).

References.

1. Duncan, M.A. *Int. J. Mass Spectrom.*, **2000**, *200*, 545.
2. Oomens, J.; Sartakov, B. G.; Meijer, G.; von Helden, G. *Int. J. Mass Spectrom.*, **2006**, *254*, 1-19.
3. MacAleese, L.; Maitre, P. *Mass Spectrom. Rev.*, **2007**, *26*, 583-605.
4. Rosenfeld, R. N.; Jasinski, J. M.; Brauman, J. I. *J. Chem. Phys.*, **1979**, *71*, 1030-1031.
5. Drzaic P. S.; Brauman, J. I. *Chem. Phys. Lett.*, **1981**, *83* 508-511.
6. Meyer, F. K.; Jasinski, J. M.; Rosenfeld, R. N.; Brauman, J. I. *J. Am. Chem. Soc.*, **1982**, *104*, 663-667.
7. Neumark, D. M.; Lykke, K. R.; Anderson, T.; Lineberger, W. C. *J. Chem. Phys.* **1985**, *83*, 4364.
8. Weber, J. M.; Robertson, W. H.; Johnson, M. A. *J. Chem. Phys.* **2001**, *115*, 10718.
9. Ayotte, P.; Bailey, C. G.; Johnson, M. A. *J. Chem. Phys.* **1998**, *108*, 444.
10. von Helden, G.; van Heijnsbergen, D.; Meijer, G. *J. Phys. Chem A*, **2003**, *107*, 1671-1688.
11. Wright, C. A.; Beauchamp, J. L. *J. Am. Chem. Soc.*, **1981**, *103*, 6499-6501.
12. Steill, J. D.; Oomens, J.; Eyler, J. R.; Compton, R. N. *submitted*.
13. Mirsaleh-Kohan, N.; Robertson, W. D.; Compton, R. N. *Mass Spec. Rev.*, **2008**, *27*, 237-285.

14. Oomens, J.; Steill, J. D. *J. Phys. Chem. A*, **2008**, *112*, 3281-3283.
15. Spinner, E. *J. Chem. Soc.*, **1964**, 4217.
16. Pike, P. R.; Sworan, P. A.; Cabaniss, S. E. *Anal. Chim. Acta*, **1993**, *280*, 253-261.
17. Rotzinger, F. P.; Kesselman-Truttmann, J. M.; Hug, S. J.; Shklover, V.; Grätzel, M. *J. Phys. Chem. B*, **2004**, *108*, 5004-5017.
18. Cabaniss, S. E.; McVey, I. F. *Spectrochim. Acta A*, **1995**, *51*, 2385-2395.
19. Woo, H. K.; Wang, X. B.; Kiran, B.; Wang, L. S. *J. Phys. Chem. A* **2005**, *109*, 11395-11400.
20. Lu, Z.; Continetti, R. E. *J. Phys. Chem. A* **2004**, *108*, 9962-9969.
21. Wang, L. S.; Ding, C. F.; Wang, X. B.; Nicholas, J. B. *Phys. Rev. Lett.* **1998**, *81*, 2667.
22. Wang, X. B.; Woo, H. K.; Kiran, B.; Wang, L. S. *Angew. Chem. Int. Ed.* **2005**, *44*, 4968-4972.
23. Wang, X. B.; Woo, H. K.; Wang, L. S.; Minofar, B.; Jungwirth, P. *J. Phys. Chem. A* **2006**, *110*, 5047-5050.
24. Wentholt, P. G.; Squires, R. R. *J. Am. Chem. Soc.* **1994**, *116*, 11890.
25. Valle, J. J.; Eyler, J. R.; Oomens, J.; Moore, D. T.; van der Meer, A. F. G.; von Helden, G.; Meijer, G.; Hendrickson, C. L.; Marshall, A. G.; Blakney, G. T. *Rev. Sci. Instrum.* **2005**, *76*, 023103.
26. Groenewold, G. S.; Oomens, J.; De Jong, W. A.; Gresham, G. L.; McIllwain, M. E.; van Stipdonk, M. J. *Phys. Chem. Chem. Phys.* **2008**, *10*, 1192-1202.
27. Oepts, D.; van der Meer, A. F. G.; van Amersfoort, P. W. *Infrared Phys. Technol.* **1995**, *36*, 297.

28. GAUSSIAN03, Revision C.02, Gaussian, Inc., Wallingford CT, 2004.
29. Spinner, E. *J. Chem. Soc. B*, **1967**, 874-879.
30. Gunion, R. F.; Gilles, M. K.; Polak, M. L.; Lineberger, W. C. *Int. J. Mass Spectrom. Ion Proc.* **1992**, 117, 601.
31. Ellison, G. B.; Engelking, P. C.; Lineberger, W. C. *J. Am. Chem. Soc.* **1978**, 100, 2556.
32. Kupser, P.; Steill, J. D.; Oomens, J.; Meijer, G.; von Helden, G. *Phys. Chem. Chem. Phys. accepted.*

	ν_a	ν_s	$\Delta\nu_{a-s}$
Benzoate			
Na salt exp. (Ref. 28)	1553	1410	143
solution (aq.) exp.(Ref. 28)	1545	1390	155
<i>solution (aq.) B3LYP/aug-cc-pVDZ</i>	1552	1313	239
gas phase exp. (Ref. 13)	1626	1311	315
<i>B3LYP/aug-cc-pVDZ</i>	1627	1311	316
Acetate			
Na salt exp. (Ref. 14)	1583	1421	162
solution (aq.) exp.(Ref. 15)	1551	1416	135
solution (aq.) exp.(Ref. 16)	1552	1415	137
<i>solution (aq.) B3LYP/aug-cc-pVDZ</i>	1554	1328	226
gas phase exp. (this work)	1590	1305	285
<i>B3LYP/aug-cc-pVDZ</i>	1603	1321	282
Propionate			
Na salt exp. (Ref. 14)	1565	1429	136
solution (aq.) exp.(Ref. 17)	1545	1413	132
<i>solution (aq.) B3LYP/aug-cc-pVDZ</i>	1557	1327	231
gas phase exp. (this work)	1600	1305	295
<i>B3LYP/aug-cc-pVDZ</i>	1604	1317	287

Table 1. Observed values for the symmetric and asymmetric carboxylate stretching frequencies in condensed and gas phases as compared to DFT calculations for the benzoate, acetate and propionate anions. All calculated harmonic frequencies are scaled by a factor of 0.98. Calculated frequencies in solution phase use the Onsager dipole model for SCF convergence. ν_a and ν_s denote the COO^- asymmetric and symmetric stretch modes.

	Benzoate			Acetate			Propionate		
	Diss.	AEA	VDE	Diss.	AEA	VDE	Diss.	AEA	VDE
<i>B3LYP/</i>									
6-31+G*	2.49	3.43	3.97	2.71	3.14	3.64	2.93	3.16	3.60
6-31+G**	2.49	3.44	3.97	2.67	3.14	3.64	2.90	3.17	3.60
6-311++G**	2.31	3.48	4.02	2.50	3.17	3.66	2.70	3.20	3.61
aug-cc-pVDZ	2.39	3.42	3.95	2.54	3.13	3.64	2.75	3.16	3.59
aug-cc-pVTZ	2.41	3.43	3.96	2.41	3.14	3.63	2.61	3.17	3.58
<i>CCD/</i>									
6-31+G*	-	-	-	2.91	3.19	3.70	-	-	-
6-31+G**	2.69	3.48	4.09	2.83	3.22	3.74	-	-	-
6-311++G**	-	-	-	2.54	3.22	3.82	-	-	-
aug-cc-pVDZ	-	-	-	2.56	3.34	3.86	2.85	3.37	3.88
<i>CCSD(T)/</i>									
6-31+G*	2.55	3.28	3.80	2.86	2.94	3.37	3.11	2.98	3.49
6-31+G**	2.52	3.30	3.81	2.79	2.97	3.40	3.04	3.01	3.52
6-311+G*	2.31	3.30	3.78	2.63	2.93	3.35	2.87	2.98	3.47
6-311++G**	2.27	3.33	3.80	2.51	2.98	3.39	2.74	3.03	-
aug-cc-pVDZ	-	-	-	2.55	3.12	3.54	2.84	3.16	-

Table 2. Calculated decarboxylation and electron detachment energies for acetate, propionate, and benzoate anions. All values are given in eV, and are zero-point energy corrected at the level of theory stated, except for CCSD(T) calculations, which are performed at B3LYP/aug-cc-pVDZ optimized structures and use the zero-point energy derived from frequencies also at this level of theory.

Adibatic Electron Affinities			
	C ₆ H ₅	CH ₃	C ₂ H ₅
<i>B3LYP/</i>			
6-31+G*	1.06	0.000	-0.32
6-31+G**	1.06	0.001	-0.30
6-311++G**	1.09	0.002	-0.24
aug-cc-pVDZ	1.09	-0.004	-0.19
aug-cc-pVTZ	0.94	-0.004	-0.20
<i>CCD/</i>			
6-31+G*	-	-0.109	-0.86
6-31+G**	-	0.019	-0.77
6-311++G**	-	0.006	-0.61
aug-cc-pVDZ	-	0.015	-0.43
<i>CCSD(T)/</i>			
6-31+G*	0.84	0.018	-0.73
6-31+G**	0.90	0.015	-0.64
6-311+G*	-	0.015	-0.64
6-311++G**	1.03	0.010	-0.48
aug-cc-pVDZ	-	0.002	-0.30

Table 3. Calculated electron affinities of CH₃, C₂H₅, and C₆H₅. All values are given in eV, and are zero-point energy corrected at the level of theory stated, except for CCSD(T) calculations, which are performed at B3LYP/aug-cc-pVDZ optimized structures and use the zero-point energy derived from frequencies also at this level of theory.

List of Figure Captions

Figure 1: IR multiple photon excitation spectrum of the benzoate anion detected simultaneously in the dissociation channel (m/z 77) and the detachment/attachment channel (to SF_6 , m/z 146). Also shown is the depletion of the benzoate parent ion, (m/z 121).

Figure 2: Comparison of detachment spectra of the benzoate anion obtained using different electron scavengers, SF_6 and CH_3I . Associative electron attachment to SF_6 produces SF_6^- ions, and dissociative electron attachment to methyl iodide results in I^- formation.

Figure 3. IR multiple photon detachment/attachment spectra of the acetate anion. Under our experimental conditions, no dissociation was observed for these species likely due to the small size and inherently slow IVR rates. The symmetric and asymmetric carboxylate stretching modes are clearly observed and correspond well to computed spectra at the B3LYP/aug-cc-pVDZ level.

Figure 4. IR multiple photon detachment/attachment spectra of the propionate anion. As for acetate, the symmetric and asymmetric carboxylate stretching modes are clearly observed and correspond well to computed spectra at the B3LYP/aug-cc-pVDZ level.

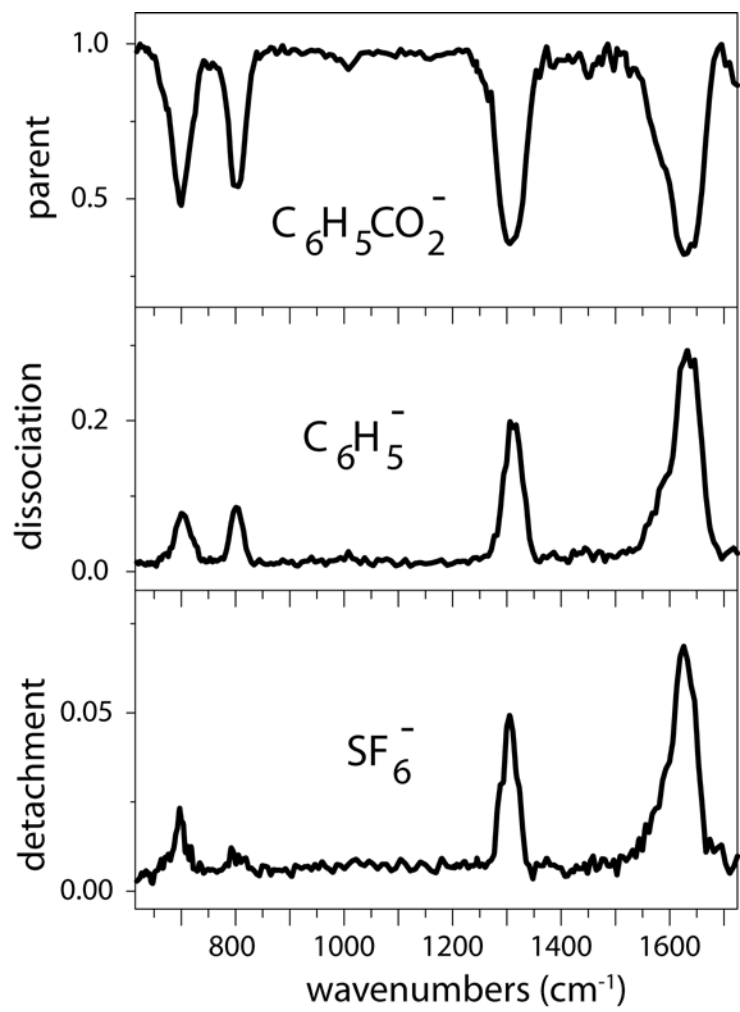


Figure 1

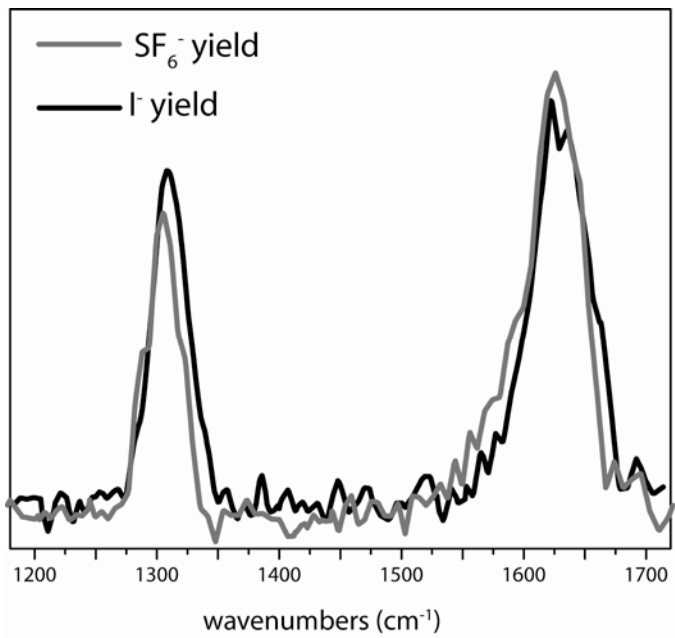


Figure 2

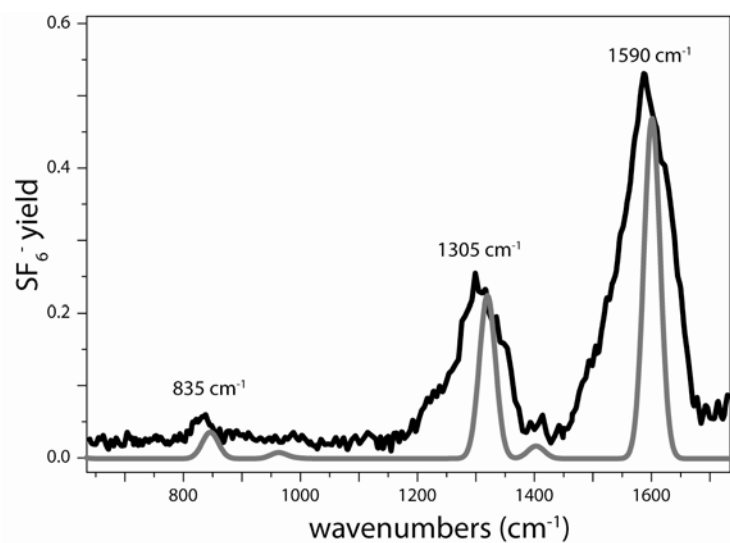


Figure 3

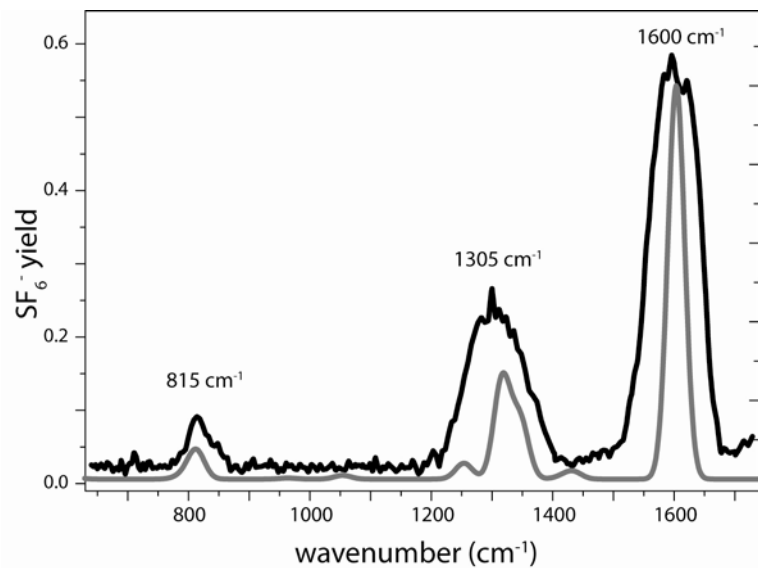


Figure 4